

Photocatalytic degradation of some VOCs in the gas phase using an annular flow reactor

Determination of the contribution of mass transfer and chemical reaction steps in the photodegradation process

A. Bouzaza*, C. Vallet, A. Laplanche

Laboratoire Rennais de Chimie et d'Ingénierie des Procédés (LARCIP), Ecole Nationale Supérieure de Chimie de Rennes, Av. Gal Leclerc, 35700 Rennes, France

Received 7 February 2005; received in revised form 9 May 2005; accepted 24 May 2005

Available online 11 July 2005

Abstract

The photodegradation of some VOCs in an annular reactor is chemical step controlled. The limitation due to mass transfer is negligible. The use of a combined plug-flow model shows that the apparent rate constant (k^*) is equal to kK representing the Langmuir–Hinshelwood rate constants. So the design of an annular reactor using the L–H model can be considered. The photodegradability of the tested VOCs is strongly dependent on the product kK . Trichloroethylene is the best degraded while toluene is the worst. The study of the mineralization rate, defined as the ultimate degradation phase of the compounds, shows that this last is firstly dependent on the contact time and not on the nature of the VOC. Moreover increasing the inlet VOC concentration leads to a decrease in the mineralization rate.
© 2005 Elsevier B.V. All rights reserved.

Keywords: Photocatalysis; Langmuir–Hinshelwood; Annular reactor; VOCs

1. Introduction

Both industrial and domestic activities are responsible of the emission of the volatile organic compounds (VOCs) [1]. Most VOCs are toxic, and some of them can be considered as carcinogenic, mutagenic or teratogenic [2]. However the most significant problem related to the emission of these pollutants is the possible production of photochemical oxidants as ozone [3]. The emissions of the VOCs also contribute to localized pollution problems.

As a consequence of these problems, VOCs have drawn considerable attention in these last years. Therefore, there is currently a great deal of interest in developing processes which can destroy these compounds [4]. Since a large number of VOCs are oxidizable, chemical oxidation processes

can be considered as a possible method. The application of heterogeneous catalytic oxidation to air pollution control is well established, as example the automotive exhaust treatments [5] and catalytic incineration [6]. However, these catalysis processes operate at elevated temperatures. Therefore, a definite need exist for developing innovative oxidative treatment methods that are prevalently applicable to most VOCs.

Photocatalytic oxidation of organic compounds in gas phase appears to be a promising process for remediation of air polluted by VOCs. Heterogeneous photocatalysis using TiO_2 has several attractions: (i) the catalyst is inexpensive, (ii) it operates at ambient temperature, (iii) the by-products are usually CO_2 and H_2O , (iv) no other chemical reagent is needed.

This process has been widely studied in the case of water treatment [7–11]. Gas-phase photocatalysis has been first explored for the degradation of trichloroethylene (TCE) when TiO_2 was irradiated with ultraviolet light [12,13]. Since then,

* Corresponding author. Tel.: +33 223238056; fax: +33 223238120.
E-mail address: abdelkrim.bouzaza@ensc-rennes.fr (A. Bouzaza).

TCE photocatalytic degradation was investigated by several authors [14–18]. However, the degradation of other classes of VOCs has received little attention [19–21] until these last years. During the last decade, the gas-phase elimination of VOCs has received more attention [22].

While the UV/TiO₂ process is an attractive technique, there are still key difficulties related to the cost and to the scale-up which will have to be overcome [23]. So the challenge of photocatalysis consists of developing reactor design with increased efficiency [24]. For the design of a continuous photocatalytic reactor, scalable to an industrial size, the most important parameters are: the catalyst configuration; the specific illuminated surface area; the mass transfer rate; the light efficiency; the UV-source and the intrinsic reaction kinetics. Various photoreactors have been developed for the treatment of VOCs in air streams: slurry reactor, packed-bed reactor, fluidized-bed reactor, fixed-bed reactor and optical fiber reactor [25]. Fixed-bed reactor, also called thin film reactor, with coated TiO₂ on the surface of the photoreactor is one of the most commonly used due to its ease on operation [26,27].

In this study, an annular photoreactor is used. The aim is to evaluate the limitation step of the VOCs photodegradation. A design equation, based on Langmuir–Hinshelwood and mass transfer model, is proposed. It can be used as the base of the photoreactor scale-up. The effects of the gas flow rate and the VOCs inlet concentration are also studied. Finally, the mineralization process, which is the ultimate step of the degradation, is approached.

2. Experimental

The VOCs used for the photodegradation were trichloroethylene (TCE), toluene, isopropanol and butane (Carlo Erba, 99% purity). No further purification of the products was done. The VOCs analysis was carried out using a gas-phase chromatograph equipped with a flame ionization detector (Fisons). The carbon dioxide produced was measured by an infrared detector (Cosma Beryl 100).

Catalyst was TiO₂ P-25 from Degussa, primary diameter: 30 nm, surface area: $50 \pm 15 \text{ m}^2 \text{ g}^{-1}$ and crystal structure: 70% anatase, 30% rutile. The TiO₂ pellets were deposited on glass fiber filter by Matrix Photocatalytic Inc. The amount of catalyst was about 2.16 g m^{-2} . Filter weaving was loose enough to let the light pass, so that all TiO₂ pellets would be illuminated.

A plug-flow annular photoreactor (Fig. 1) made up of two stainless steel tubes (L : 2 cm \times 160 cm, $\varnothing_{\text{internal}}$: 4 cm) supplied by Matrix Photocatalytic Inc. was used. During experiments, only the first tube was photocatalytically active. Illumination was provided by a 150 W low pressure mercury lamp with a maximum wavelength at 254 nm. The UV lamp was located at the center of the cylinder and was protected by a quartz tube; 0.18 m^2 of photocatalytic support was fixed on the quartz tube. Finally, the effective gas volume in the active tube was 0.25 dm^3 , so the ratio (filter surface)/(reactor

volume) equals to 720 m^{-1} . The thickness of the gas film was equal to 4 mm.

2.1. Experimental procedure

The ambient air was used as a gas carrier. Its relative humidity was about 45–50% and the temperature was at $20 \pm 2^\circ \text{C}$. The concentration of the VOC in the contaminated atmosphere was obtained by vaporization of organic compounds using predetermined values of flow rate. The VOC vapor was then extracted. The temperature of the solvent-containing bottle was maintained constant for providing VOCs vapor with a steady concentration. Then the “secondary” flow air was mixed to the main stream.

When the VOC were gaseous at ambient temperature, as butane, the secondary flow gas was mixed directly to the main stream.

In a typical test, a contaminated air stream was passed through the photoreactor in the absence of UV illumination until the gas–solid adsorption equilibrium was established. This dark equilibration process provides a qualitative indication of the adsorption affinity between the catalyst and the VOC. After the adsorption process reached equilibrium (depending upon the nature of the VOC, the flow rate and the concentration), as indicated by identical inlet/outlet VOC concentration, the UV illumination was turned on and the outlet gas was sampled at regular intervals. A new steady state was achieved about 30–60 min after the light was turned on. After completing the experiments, the reactor was flushed under UV illumination for 1 h using clean air.

N.B.: The direct photolysis of toluene and other VOCs at 254 nm was found to be trivial by some authors [22,28].

3. Results and discussion

3.1. Toluene photodegradation

3.1.1. Determination of the limiting step

Whereas the mass transfer rate could be very large and not limiting for a batch reactor [29], the rate would be finite and limiting in the case of the continuous reactor. When the tubular reactor is used, it would be interesting to know if the mass transfer rate or the kinetic is the limiting step.

Overall mass balances on the gas phase and the solid phase, in a continuous reactor at steady state, give the following equations [30]:

- Gas phase:

$$u \frac{\partial C}{\partial Z} + k_m a_v (C - C_s) = 0 \quad (1)$$

- Solid phase:

$$k_m a_v (C - C_s) = k \frac{KC_s}{1 + KC_s} \quad (2)$$

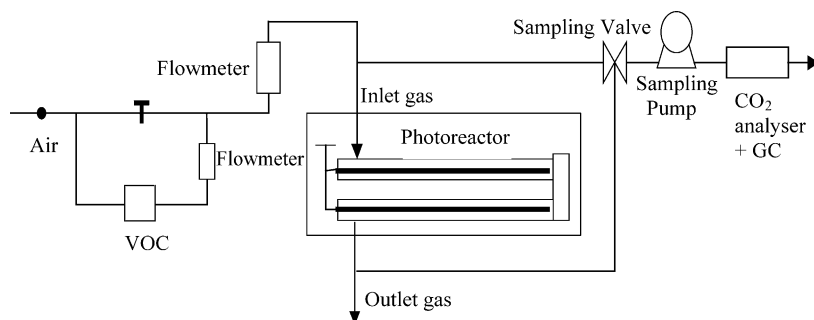


Fig. 1. Experimental set up.

In the above equations, C is the bulk gas-phase concentrations, C_S represents the concentration near the surface of the photocatalyst. A Langmuir–Hinshelwood mechanism is assumed for the degradation of the VOC. This was established in a previous study concerning the toluene [29] and this is the case for the major VOCs [31].

Usually we can assume that $KC_S < 1$. Under these conditions the solid phase mass balance can be approximated to:

- Solid phase:

$$k_m a_v (C - C_S) = k K C_S \quad (3)$$

Using Eq. (3) to obtain C_S and substituting in Eq. (1) and solving the resulting differential equation, we obtain the following solution [30]:

$$\frac{C_S}{C_F} = \exp\left(-k^* \frac{L}{u}\right) \quad (4)$$

where k^* represents the apparent rate constant (min^{-1}), L the length of the reactor, C_F the inlet concentration and u the velocity of the gas through the reactor.

The product $k^* L/u$ is known as the reaction Damkohler number and is dimensionless. k^* takes into account both the rate of the reaction at the surface of the immobilized catalyst and the mass transfer of the reactant to the surface.

k^* is given by the following equation:

$$\frac{1}{k^*} = \frac{1}{kK} + \frac{1}{k_m a_v} \quad (5)$$

where k is the reaction rate constant ($\text{mol l}^{-1} \text{min}^{-1}$), K the Langmuir adsorption constant (l mol^{-1}), k_m the mass transfer coefficient from gas to catalyst surface (m min^{-1}) and a_v the total effective catalyst area per unit volume of the reactor ($\text{m}^2 \text{m}^{-3}$). In Eq. (5), the two terms on the right-hand represent respectively the reaction rate and mass transfer resistance.

Eq. (4) can be used to obtain the apparent rate constant k^* from known experimental values of C_S/C_F at given flow velocity u . The value of C_S is assumed to be equal to the outlet concentration.

If we suppose that the mass transfer is not the limiting step and that the effect of intermediate product is negligible, then

the degradation rate in a plug-flow reactor can be expressed as

$$u \frac{dC}{dZ} = -\frac{kKC}{1+KC} \quad (6)$$

where Z represents the axial position in the photoreactor (m). After rearrangement, integration of Eq. (6) for the entire reactor length (L) leads to [25]:

$$\frac{\ln(C_F/C_S)}{C_F - C_S} = \frac{kKL}{u(C_F - C_S)} - K \quad (7)$$

If the proposed L–H model is valid, a plot of $\ln(C_F/C_S)/(C_F - C_S)$ versus $1/(C_F - C_S)$ should be linear. The slope should be equal to kKL and the negative intercept with ordinate axis equal to $-K$.

Then the comparison between the value of kK and k^* obtained respectively from Eqs. (7) and (4) will be done. This will allow us to estimate the effect of mass transfer resistance on the photodegradation of the VOCs.

3.2. Continuous photodegradation of the toluene

The regression of experimental results using the L–H model is represented in Fig. 2. The data appears scattered even if the maximum experimental error is taken into account. This is probably due to the fact that the influence of intermediate products is not negligible. This data dispersion can also be due to the effect of the mass transfer. This will be discussed later. However, the continuous degradation of

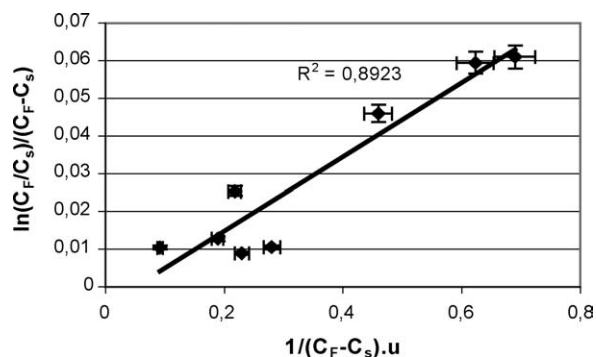


Fig. 2. Regression of experimental results with Eq. (7).

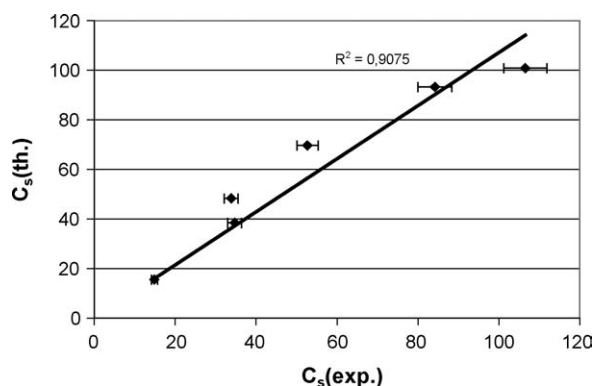


Fig. 3. Comparison between the experimental and the predicted outlet concentration (C_F varies from 20 to 100 mg m^{-3} , gas flow rate = 1 $\text{m}^3 \text{h}^{-1}$).

toluene in a plug-flow reactor can be represented by L–H model.

The values of L–H rate constant and Langmuir adsorption constant, obtained from the linear regression, are $k = 13.39 \text{ mg m}^{-3} \text{ s}^{-1}$ and $K = 0.0049 \text{ m}^3 \text{ mg}^{-1}$. These values are different from those obtained in a previous work on the batch reactor [29]. The L–H rate constant is about three times higher in the continuous plug-flow reactor, whereas the Langmuir adsorption constant is three times less. It is interesting to note that the degradation rate is dependent on the product kK , which is the same for batch and continuous reactors studied. Therefore a higher adsorption constant does not always result in a higher degradation rate.

Eq. (7) can be used as a design model to predict the outlet concentration in a plug-flow reactor. Fig. 3 shows the comparison between the experimental and calculated outlet concentration for a given gas flow rate. The kinetic step seems to be the limited step for the photodegradation of the toluene. Moreover, the design equation (Eq. (7)) can be used to determine the reactor length required to achieve a desired degradation rate.

Nevertheless, it would be useful to obtain the apparent rate constant k^* from experimental values and to compare the influence of different parameters such as toluene concentration and flow rate. The apparent rate constant k^* will be compared to the reaction rate constant (Table 1).

We note that the ratio k^*/kK approaches 1, the overall mass transfer is equal to the reaction rate constant (kK) even if the flow velocity is low. The mass transfer step is not the limited step, the photodegradation of the toluene is reaction rate controlled in the plug-flow reactor. Using the semi-empirical L  v  que equation [32], the mass transfer coefficient (k_m) was evaluated. The values obtained were about 10–100 times higher than k^* . This confirms that the resistance ($1/k_m a_v$) due

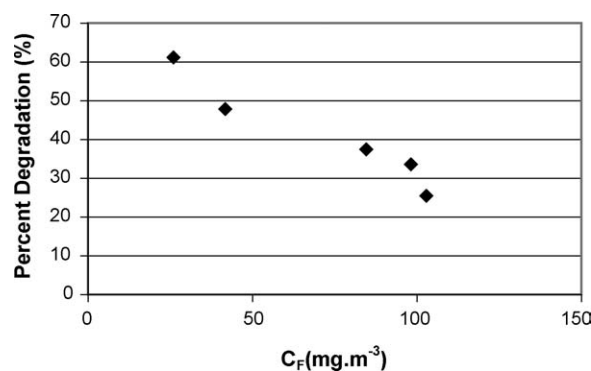


Fig. 4. Evolution of the degradation rate vs. inlet concentration (gas flow rate = 0.2 $\text{m}^3 \text{h}^{-1}$).

to the mass transfer is negligible. It is interesting to note that in the liquid phase, when using tubular reactor, Dijkstra et al. [24] give a value of mass transfer coefficient about 100 times less.

N.B.: Some ratio values given in Table 1 are sometimes less than 1. For example, for the same flow velocity (0.23–0.25), the ratio varies from 0.38 to 1.02. The same observation can be made concerning the flow velocity values 0.48 and 0.51.

This is probably due, in our point of view, to the “flow instability”. The Reynolds number varies from 57 to 292 for the highest flow velocity. Even if the flow is laminar some localized turbulences can appears due to the roughness of the catalytic media, and this leads to the improvement of the mass transfer. The appearance of these turbulences being random, this can explain the differences observed.

3.3. Effect of the inlet concentration on the toluene degradation

The degradation of toluene decreases when the inlet concentration increases (Fig. 4). This can be due to the limited amount of the active sites on the surface of TiO_2 available for the adsorption of toluene before the decomposition. Similar results were observed by many authors [25]. The experimental results can be correlated by the L–H rate equation. Because the inlet concentration is low, the L–H kinetic equation could be reduced to a pseudo-first order rate equation:

$$\ln \left(\frac{C_F}{C_S} \right) = k_1 \tau \quad (8)$$

where k_1 is the pseudo-first-order rate constant, and τ the retention time.

3.4. Photodegradation of isopropyl alcohol, TCE and butane

The study of the photodegradation of other VOCs has been carried out on the same plug-flow reactor. The L–H model is used to represent the experimental results obtained. The other VOCs studied are isopropyl alcohol, trichloroethylene (TCE) and butane.

Table 1

Values of overall mass transfer (k^*) and the ratio k^*/kK

$u \text{ (m s}^{-1}\text{)}$	0.10	0.23	0.25	0.25	0.46	0.46	0.48	0.51
$k^* \text{ (s}^{-1}\text{)}$	0.06	0.07	0.05	0.03	0.08	0.06	0.08	0.03
k^*/kK	0.97	1.02	0.69	0.38	1.16	0.90	1.19	0.40

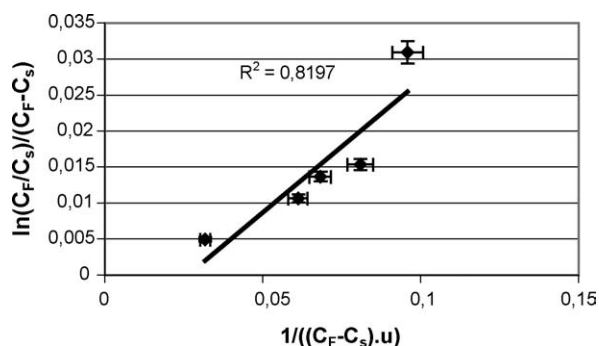


Fig. 5. Photocatalytic degradation of isopropyl alcohol (C_F varies from 100 to 200 mg m^{-3}).

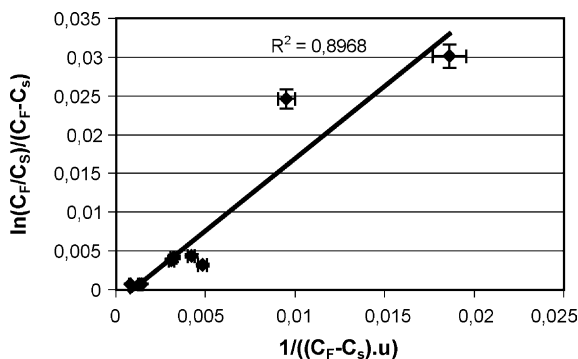


Fig. 6. Photocatalytic degradation of TCE (C_F varies from 100 to 2000 mg m^{-3}).

The experimental results and the L–H model are represented in Figs. 5–7.

We note that for all the VOCs, the kinetic step seems to be the limited step. The L–H model gives a correct correlation with the experimental results. The values of the L–H constants are given in Table 2.

As we reported above, the degradation rate is dependent on k and K . A lower adsorption constant does not always result in a lower degradation rate. For example, it can be seen (Table 2) that TCE had the lower adsorption constant but is the most degraded constituent. And toluene, even if its adsorption constant is not the lowest, is the least degraded. The L–H

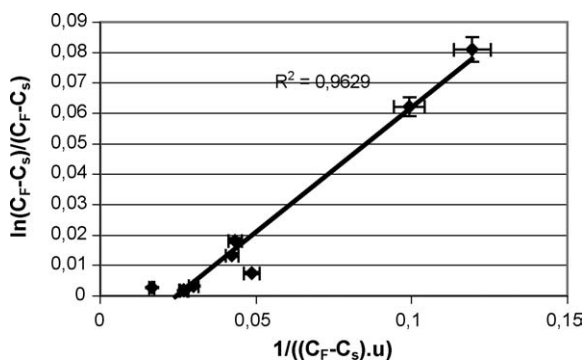


Fig. 7. Photocatalytic degradation of the butane (C_F varies from 80 to 500 mg m^{-3}).

Table 2

Values of the L–H constants model

VOC	k ($\text{mg m}^{-3} \text{s}^{-1}$)	K ($\text{m}^3 \text{mg}^{-1}$)	kK (s^{-1})
Isopropyl alcohol	25.382	0.0096	0.244
TCE	729.254	0.0017	1.240
Butane	27.461	0.0199	0.546
Toluene	13.388	0.0049	0.066

rate constant (k) seems to be the predominant parameter in the photodegradation of the VOCs studied. Toluene, as an aromatic compound is the least degraded. TCE is the most degraded even if its molecular structure is double bonded. This can be due to the fact that this compound absorbs 254 nm irradiation. So some photolysis of TCE occurs and this leads to the formation of free radicals Cl^\bullet which accelerate the reaction [33,34]. The photocatalysis leads also to the formation of Cl^\bullet .

3.5. Mineralization

The experimental quantity of the produced carbon dioxide is compared to the theoretical. This last is the quantity which can be obtained if the VOC degradation is complete, i.e. leads to the formation of carbon dioxide, water and minerals. For example, when one mole of butane is degraded it will lead to the formation of four moles of carbon dioxide.

We note that for all the VOCs, the mineralization rate (Fig. 8) is hardly dependent on the inlet gas flow rate. The mineralization rate decreases when the gas flow increases. Indeed the increasing inlet gas flow leads to less contact time then the complete degradation cannot occur. The mineralization rate varies from high value (>80%), at the low flow rate, to less value (<30%) at the high flow rate. Except butane, the nature of the VOCs seems not to have a significant effect. The mineralization rate is strongly dependent on the contact time.

Furthermore, in the experiments carried out with different inlet VOCs concentrations, we note (Fig. 9) that the mineralization rate decreases when increasing inlet concentration. The competitive effect between the by-product and the initial constituent can explain this behavior. Indeed the number of

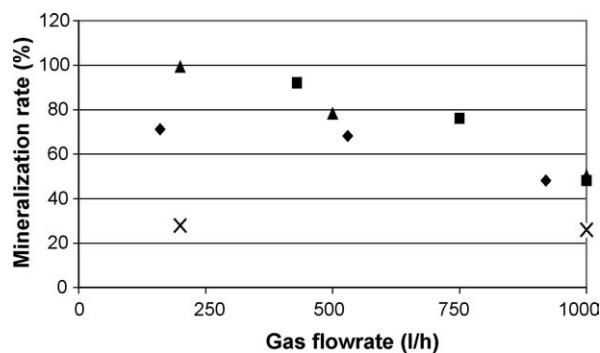


Fig. 8. Rate of VOCs mineralization vs. inlet gas flow rate: (◆) toluene; (■) isopropyl alcohol; (▲) TCE; (×) butane.

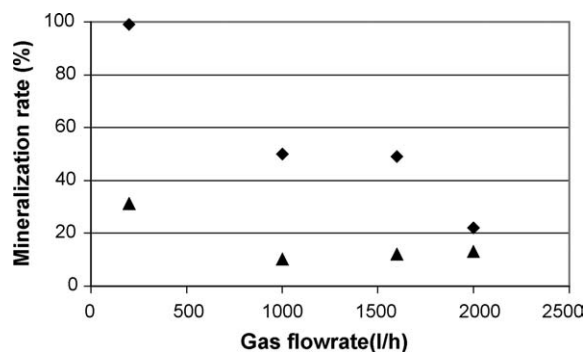


Fig. 9. Effect of the inlet TCE concentration on the mineralization rate: (◆) $C_F = 100 \text{ mg m}^{-3}$; (▲) $C_F = 2000 \text{ mg m}^{-3}$.

active sites was constant, when the inlet VOC concentration increase, the competition between this last and by-products increases. This leads to a desorption of the by-products and then to a decrease in the mineralization rate. A follow-up in concentration of the by-products, in the effluent, would make it possible to confirm this assumption. Unfortunately this could not be done.

At high flow rate, the mineralization rate becomes independent on the inlet concentration. In other words, the contact time becomes the prevalent factor. The behavior is the same for all the VOCs.

4. Conclusion

The photodegradation of some VOCs in a plug-flow reactor was studied. The limited step of the process is the chemical one. The use of Langmuir–Hinshelwood model gives a good correlation of the experimental results and allows us to determine the reaction rate constant k and the adsorption constant K . The photodegradation of the VOCs depends on the product kK . The TCE were the best degraded probably due to the formation of free radical Cl^\bullet while toluene were the least.

A model based on a combination of mass transfer and chemical steps was used to correlate the experimental results. The comparison of the apparent rate constant (k^*) and the product kK made it possible to confirm that the limited step of the process is the chemical reaction. The L–H model, adapted to the plug-flow reactor, can be used to design and scale-up the photocatalytic reactors.

The study of the mineralization rate of the VOCs shows that the predominant parameter is the contact time. The nature of the VOCs has no significant effect on the mineralization. A complete study with identification of the by-products will give more information concerning the photodegradation of the cited VOCs.

References

- [1] K. Wolf, A. Yazdani, P. Yates, J. Air Waste Manage. Assoc. 41 (1991) 1055.
- [2] C.F. Wilkinson, Environ. Sci. Technol. 22 (1988) 1381.
- [3] S.M. Japer, T.J. Wallington, S.J. Rudy, T.Y. Chang, Environ. Sci. Technol. 25 (1991) 415.
- [4] R.M. Alberici, W.F. Jardim, Appl. Catal. B: Environ. 14 (1997) 55.
- [5] J.N. Armor, Appl. Catal. B: Environ. 1 (1992) 221.
- [6] M. Kosuko, C.M. Nunez, J. Air Waste Manage. Assoc. 40 (1990) 244.
- [7] D.F. Ollis, Environ. Sci. Technol. 19 (1985) 480.
- [8] D.F. Ollis, E. Pelizzetti, N. Serpone, in: N. Serpone, E. Pelizzetti (Eds.), Photocatalysis: Fundamentals and Applications, Wiley, New York, 1989, p. 604.
- [9] D.F. Ollis, E. Pelizzetti, N. Serpone, Environ. Sci. Technol. 25 (1991) 1522.
- [10] J.M. Herrmann, C. Guillard, P. Pichat, Catal. Today 17 (1993) 7.
- [11] A. Mills, R.H. Davies, D. Worsley, Chem. Soc. Rev. 22 (1993) 417.
- [12] L.A. Dibble, G.B. Raupp, Catal. Lett. 4 (1990) 345.
- [13] L.A. Dibble, G.B. Raupp, Environ. Sci. Technol. 26 (1992) 492.
- [14] L.A. Phillips, G.B. Raupp, J. Mol. Catal. 77 (1992) 297.
- [15] S. Yamazaki-Nishida, K.J. Nagano, L.A. Phillips, S. Cervera-March, M.A. Anderson, J. Photochem. Photobiol. A: Chem. 70 (1993) 95.
- [16] S. Kutsuna, Y. Ebihara, K. Nakamura, T. Ibusuki, Atmos. Environ. A 27 (1993) 599.
- [17] M.R. Nimlos, W.A. Jacoby, D.M. Blake, T.A. Milne, Environ. Sci. Technol. 27 (1993) 732.
- [18] W.A. Jacoby, M.R. Nimlos, D.M. Blake, Environ. Sci. Technol. 28 (1994) 1661.
- [19] N.N. Lichtin, J. Dong, K.M. Vijayakumar, Water Pollut. Res. J. Canada 27 (1992) 203.
- [20] G.B. Raupp, T.C. Junio, Appl. Surf. Sci. 72 (1993) 321.
- [21] T.N. Obee, R.T. Brown, Environ. Sci. Technol. 29 (1995) 1223.
- [22] Z. Pengyi, L. Fuyan, Y. Gang, C. Qing, Z. Wanpeng, J. Photochem. Photobiol. A: Chem. 156 (2003) 189.
- [23] H. Ibrahim, H. Lasa, Ind. Eng. Chem. Res. 38 (1999) 3211.
- [24] F.J. Dijkstra, H. Buwalda, A.W.F. de Jong, A. Michorius, J.G.M. Winkelman, A.A.C. Beenackers, Chem. Eng. Sci. 56 (2001) 547.
- [25] Y. Ku, C.-M. Ma, Y.-S. Shen, Appl. Catal. B: Environ. 34 (2001) 181.
- [26] C.H. Hung, B.J. Marinas, Environ. Sci. Technol. 31 (1997) 562.
- [27] J.M. Herrmann, H. Tahiri, Y. Aitichou, G. Lassaletta, E.A.R. Gonzalez, A. Fernandez, Appl. Catal. B: Environ. 13 (1997) 219.
- [28] Y.-S. Shen, Y. Ku, Chemosphere 38 (8) (1999) 1855.
- [29] A. Bouzaza, A. Laplanche, J. Photochem. Photobiol. A: Chem. 150 (2002) 207.
- [30] H.F. Lin, R. Ravikrishna, K.T. Valsaraj, Sep. Purif. Technol. 28 (2002) 87.
- [31] A. Mills, S. Le Hunte, J. Photochem. Photobiol. A: Chem. 108 (1997) 1.
- [32] R.B. Bird, W.E. Stewart, E.N. Lightfoot, Transport Phenomena, Wiley, New York, 1960.
- [33] H. Lin, S. Cheng, J. Zhang, C. Cao, W. Jiang, Chemosphere 35 (12) (1997) 2881.
- [34] C. Feiyan, S.O. Pehkonen, M.B. Ray, Water Res. 36 (2002) 4203.